An extension to the Frenet-Serret and Bishop invariant extended Kalman filters for tracking accelerating targets

Joe Gibbs
James Watt School of Engineering
University of Glasgow
Glasgow, UK
j.gibbs.1@research.gla.ac.uk

David Anderson
James Watt School of Engineering
University of Glasgow
Glasgow, UK
dave.anderson@glasgow.ac.uk

Matt MacDonald
Sightline Control Systems group
Leonardo UK
Edinburgh, UK
matt.macdonald@leonardo.com

John Russell
Sightline Control Systems group
Leonardo UK
Edinburgh, UK
john.russell@leonardo.com

***Abstract*—This paper presents an extension to the original Frenet-Serret and Bishop frame target models used in the invariant extended Kalman filter (IEKF) to account for tangential accelerations for highly-manoeuvrable targets. State error propagation matrices are derived for both IEKFs and used to build the accelerating Frenet-Serret (FSa-LIEKF) and Bishop (Ba-LIEKF) algorithms. The filters are compared to the original Frenet-Serret and Bishop algorithms in a tracking scenario featuring a target performing a series of complex manoeuvres. The accelerating forms of the LIEKF are shown to improve velocity estimation during non-constant velocity trajectory segments at the expense of increased noise during simpler manoeuvres.**

***Index Terms*—Frenet-Serret, Bishop frame, Kalman filter, Lie groups**

I. Introduction

Target tracking is the problem of estimating rigid body motions in 3D space that a target undergoes during motion. Traditional nonlinear state estimation algorithms such as the extended (EKF), Unscented (UKF) [1] and cubature Kalman filters (CKF) [2] use models with changes in velocity or acceleration modelled as Gaussian white noise to track manoeuvring targets. Other models such as the Singer acceleration model [3] are common in industrial radar systems with [4] providing a comprehensive review. For manoeuvring targets, a bank of filters are run in a multiple model algorithm such as the interacting multiple model IMM [5] with a Kalman filter running each model before fusing the results. Simpler dynamic models incorporating the kinematics of 3D curves have been proposed to provide a more general dynamic model for target tracking. The Frenet-Serret left-invariant extended Kalman filter (FS-LIEKF) first presented in [6] estimates the pose $\chi_t \in SE(3)$ of a target along with scalar parameters describing the shape and motion of the trajectory. The Frenet-Serret formulae are used to propagate the target pose since they provide a concise means of characterising smooth curves γ, in this case the target trajectory, in 3D space ($\gamma \in \mathbb{R}^3$) through the formulae in equation (1). The Frenet-Serret equations are an elegant framework for tracking as they, by definition, describe the motion of curves. This is beneficial for tracking scenarios where the observer is attempting to reconstruct or predict a curved trajectory by propagating a set of equations. With a set of scalar Frenet parameters, a wide range of curves can be extrapolated, from simple straight segments to helices and spirals.

$$\begin{bmatrix} \dot{\mathbf{T}} \\ \dot{\mathbf{N}} \\ \dot{\mathbf{B}} \end{bmatrix} = u \begin{bmatrix} 0 & \kappa & 0 \\ -\kappa & 0 & \tau \\ 0 & -\tau & 0 \end{bmatrix} \begin{bmatrix} \mathbf{T} \\ \mathbf{N} \\ \mathbf{B} \end{bmatrix} \tag{1}$$

Bishop showed that the Frenet-Serret frame is the not the only frame that can be readily applied to curves, extending the Frenet equations to be globally defined [7] with two signed curvatures rather than a single curvature and torsion. While the Frenet frame defines the true geometry of the space curve, with the unit normal vector N pointing towards the centre of curvature in the osculating plane, the Bishop formulae, shown in (2), enable us to initialise any starting attitude with the development equations valid for any frame. This is the case as the Bishop frame is not unique for a given curve [7].

$$\begin{bmatrix} \dot{\mathbf{T}} \\ \dot{\mathbf{M}}_1 \\ \dot{\mathbf{M}}_2 \end{bmatrix} = u \begin{bmatrix} 0 & \kappa_1 & \kappa_2 \\ -\kappa_1 & 0 & 0 \\ -\kappa_2 & 0 & 0 \end{bmatrix} \begin{bmatrix} \mathbf{T} \\ \mathbf{M}_1 \\ \mathbf{M}_2 \end{bmatrix} \tag{2}$$

The Bishop or parallel transport frame has previously been used to define tracking problems and has been implemented within an invariant extended Kalman filter for tracking a manoeuvring target with radar measurements [8], using the framework laid out by Pilte et al. [6], [9]. Both approaches are well suited to tracking problems given the ability to define complex curves using slow changing or even constant

parameters. While the curvature $\hat{\kappa}_t$ and torsion $\hat{\tau}_t$ parameters of the Frenet-Serret apparatus in the FS-LIEKF of [6] are able to account for the twisting motion of trajectories, tangential accelerations cannot be estimated and the filter relies upon process noise on the norm velocity $\hat{u}_t$ and unit tangent vector T to estimate the magnitude and direction. The same is true for the Bishop frame implementation or B-LIEKF, albeit with the replacement of curvature and torsion with the two Bishop curvatures $\hat{\kappa}_1$, $\hat{\kappa}_2$. This extension was originally noted by Pilte [10] with the warning that the acceleration would degrade performance on trajectories with constant velocity segments, similar to the results seen when comparing simple CV and CA EKFs.

With more modern targets able to manoeuvre with high accelerations it is critical to have a kinematic model that can adapt well to large changes in velocity. This paper presents the extension to the Frenet-Serret and Bishop IEKF algorithms to account for accelerating targets. The state error propagation matrix for the Bishop implementation is derived and a short simulation is produced to highlight the improved performance during components of trajectories with non-constant velocity.

II. Frenet-Serret and Bishop Acceleration LIEKFs

The invariant extended Kalman filter (IEKF) is a recent extension to the Kalman filter that enables the definition of state spaces on matrix Lie groups [11]. The key advantage of the IEKF is that by defining a left or right-invariant estimation error, the linearisation is performed on independent error dynamics. This ensures that the computed Kalman gain is not dependent on the accuracy of the current state estimate and hence convergence can be guaranteed for a wider range of trajectories [12]. Barrau and Bonnabel present a complete introduction to the IEKF in [13] with the Unscented variant covered in [14]. The non-accelerating form of the Frenet-Serret process model can be found in [6], [9]. Here, the attitude of the target is expressed as the Frenet-Serret or Bishop rotation matrix R_t as in [6]. The only change is to assume that an acceleration a_t acts on the target to update the norm velocity u_t. Changes in this acceleration, referred to as jerk, are modelled as Gaussian white noise. The equivalent Bishop frame dynamics are written as (3), substituting the curvature and torsion for the first and second Bishop curvatures κ_1, κ_2

$$\frac{d}{dt}\mathbf{x} = \begin{cases} \frac{d}{dt}R_t = R_t[\omega_{b,t} + w_t^{\omega}]_\times \in SO(3) \\ \frac{d}{dt}x_t = R_t(v_t + w_t^x) \in \mathbb{R}^3 \\ \frac{d}{dt}\kappa_t^1 = w_t^{\kappa^1} \in \mathbb{R}^1 \\ \frac{d}{dt}\kappa_t^2 = w_t^{\kappa^2} \in \mathbb{R}^1 \\ \frac{d}{dt}u_t = a_t + w_t^u \in \mathbb{R}^1 \\ \frac{d}{dt}a_t = w_t^a \in \mathbb{R}^1 \end{cases} \tag{3}$$

The target velocity v_t acts only in the tangential direction $v_t = \begin{bmatrix} u_t & 0 & 0 \end{bmatrix}^T$ and the Bishop Darboux vector is written as $\omega_{b,t} = \begin{bmatrix} 0 & -\kappa_2 & \kappa_1 \end{bmatrix}^T$. Note that since the filter estimates the target attitude, process noise for the position is only added in the tangential direction, that is $w_t^x = \begin{bmatrix} w_t^x & 0 & 0 \end{bmatrix}^T$. The state space is defined as $SE(3) \times \mathbb{R}^4$ which we will refer to as the manifold, noting that, since only part of the state is an element of the special Euclidean Lie group of 3D rigid body motion $SE(3)$, one cannot fully implement the IEKF [6]. The convergence guarantees presented in [12] are not valid for filters defined on mixed Lie group states however the IEKF still provides an elegant method for incorporating group constraints associated with common matrix Lie groups such as $SE(3)$. Additionally, the nature of the Frenet and Bishop formulae means that, in situations where the filter runs at frequency exceeding the measurement availability, the propagation is better suited to a wider range of trajectories.

A. IEKF Algorithm

This paper provides the key stages in deriving the state error propagation matrix for the Ba-LIEKF, but the same method can be easily applied to the Frenet-Serret case. To propagate the state error covariance we must first linearise the error dynamics. From [6], the state errors are defined as (4), a combination of left-invariant state error and linear vector error.

$$\eta = \begin{cases} \chi_t^{-1}\hat{\chi} \\ \hat{\zeta} - \zeta_t \end{cases} = \begin{bmatrix} \eta_t^R \\ \eta_t^x \\ \eta_t^{\kappa_1} \\ \eta_t^{\kappa_2} \\ \eta_t^u \\ \eta_t^a \end{bmatrix} = \begin{bmatrix} R_t^T\hat{R}_t \\ R_t^T(\hat{x}_t - x_t) \\ \hat{\kappa_{1t}} - \kappa_{1t} \\ \hat{\kappa_{2t}} - \kappa_{2t} \\ \hat{u}_t - u_t \\ \hat{a}_t - a_t \end{bmatrix} \tag{4}$$

With the true trajectory formed from the Bishop formulae in (3) and the noise-free filter models we can derive the error dynamics. Since Pilte et al. present this process for the Frenet-Serret formulae in [6] we proceed with the Bishop case. The time derivative of the error dynamics can be shown to be

$$\frac{d}{dt}\eta_t = \begin{bmatrix} -[\omega_{b,t} + w_t^{\omega}]_\times \eta_t^R + \eta_t^R[\hat{\omega}_{b,t}]_\times \\ -[\omega_{b,t} + w_t^{\omega}]_\times \eta_t^x + v_t + w_t^u - \eta_t^R\hat{v}_t \\ -w_t^{\kappa_1} \\ -w_t^{\kappa_2} \\ \eta_t^a - w_t^u \\ -w_t^a \end{bmatrix} \tag{5}$$

This can then be linearised using a first-order approximation which is shown by Barrau and Bonnabel to be exact [12]. The position and $\mathbb{R}^4$ states are assumed to follow $\xi_t = \eta_t$ while the rotation matrix R_t, an element of the special orthogonal group of 3D rotations $SO(3)$, follows a first order approximation of the exponential map for $SO(3)$, that is $\eta_t^R \approx I_3 + [\xi_t^R]_\times$. Substituting our linearised error definitions into equation (5) gives the linearised error equations shown in (6).

$$\frac{d}{dt}\xi_t = \begin{bmatrix} -[\omega_{b,t} + w_{b,t}^{\omega}]_\times (I_3 + [\xi_t^R]_\times) + (I_3 + [\xi_t^R]_\times)[\hat{\omega}_{b,t}]_\times \\ -[\omega_{b,t} + w_t^{\omega}]_\times \xi_t^x + v_t + w_t^u - (I_3 + [\xi_t^R]_\times)\hat{v}_t \\ -w_t^{\kappa_1} \\ -w_t^{\kappa_2} \\ \xi_t^a - w_t^u \\ -w_t^a \end{bmatrix} \tag{6}$$

By rearranging into the form $\dot{\xi}_t = A\xi_t + w_t$ with $w_t = \begin{bmatrix} w_t^{\omega} & w_t^x & w_t^{\kappa_1} & w_t^{\kappa_2} & w_t^u & w_t^a \end{bmatrix}^T$, the state error propaga-

tion matrix A_t for the accelerating Bishop equations can be derived as (7).

$$A_t = -\begin{bmatrix} 0 & -\hat{\kappa}_1 & -\hat{\kappa}_2 & 0 & 0 & 0 & 0 & 0 & 0 & 0 \\ \hat{\kappa}_1 & 0 & 0 & 0 & 0 & 0 & 0 & 1 & 0 & 0 \\ \hat{\kappa}_2 & 0 & 0 & 0 & 0 & 0 & -1 & 0 & 0 & 0 \\ 0 & 0 & 0 & 0 & -\hat{\kappa}_1 & -\hat{\kappa}_2 & 0 & 0 & -1 & 0 \\ 0 & 0 & -\hat{u}_t & \hat{\kappa}_1 & 0 & 0 & 0 & 0 & 0 & 0 \\ 0 & \hat{u}_t & 0 & \hat{\kappa}_2 & 0 & 0 & 0 & 0 & 0 & 0 \\ 0 & 0 & 0 & 0 & 0 & 0 & 0 & 0 & 0 & 0 \\ 0 & 0 & 0 & 0 & 0 & 0 & 0 & 0 & 0 & 0 \\ 0 & 0 & 0 & 0 & 0 & 0 & 0 & 0 & 0 & -1 \\ 0 & 0 & 0 & 0 & 0 & 0 & 0 & 0 & 0 & 0 \end{bmatrix} \tag{7}$$

It can be seen that for the state error propagation matrix in equation (7), the only change from the non-accelerating case in [6] is the addition of -1 in the final column. This can be repeated for the equivalent Frenet-Serret model by taking the A matrix from [6] and adding the final row and column from equation (7).

1) Propagation

With the state error propagation matrix derived, the complete IEKF algorithm can be implemented by first propagating the state using the Frenet-Serret and Bishop equations in [6] and equation (3). The error covariance can then be propagated using equation (8)

$$P_{k|k-1} = \Phi_k P_{k-1|k-1} \Phi_k^T + \check{Q}_k \tag{8}$$

where $\Phi_k = \exp_m(A_t \Delta t)$ and $\check{Q}_k \approx \Phi_k Q \Phi_k^T \Delta t$.

2) Update Equations

The FSa-LIEKF and Ba-LIEKF update step follows as equations (9) to (10)

$$K_k = P_{k|k-1} \tilde{H}_k^T (\tilde{H}_k P_{k|k-1} \tilde{H}_k^T + N_k^R)^{-1} \tag{9}$$

where $\tilde{H}_k$ is the measurement Jacobian of the spherical to Cartesian transformation rotated into the target frame as per [8], [10]. The error covariance is updated using the standard Kalman equation, although the Joseph form is recommended to avoid numerical issues associated with round-off errors.

$$P_{k|k} = (I_{10} - K_k \tilde{H}_k) P_{k|k-1} \tag{10}$$

Due to the composition of the state as a mixed manifold, the state update uses the boxplus $\oplus$ operator to correct the state.

$$\hat{\mathbf{x}}_{k|k} = \hat{\mathbf{x}}_{k|k-1} \oplus K_k (Y_n - h(\hat{\mathbf{x}}_{k|k-1})) \tag{11}$$

This box-plus operator refers to the composition of a tangent-space element onto the manifold, with the $\ominus$ performing the opposite operation. These retain the left or right bias and as such we use the left $\oplus$ to update the state. This results in two separate operations for the $SE(3)$ Lie group and $\mathbb{R}^4$ vector components as shown in equation (12).

$$\begin{cases} \hat{\chi}_{k|k} = \hat{\chi}_{k|k-1} \exp_{SE(3)}(K_k^{\chi}(Y_n - h(\hat{\chi}_{k|k-1}))) \\ \hat{\zeta}_{k|k} = \hat{\zeta}_{k|k-1} + K_k^{\zeta}(Y_n - h(\hat{\chi}_{k|k-1})) \end{cases} \tag{12}$$

Here the Lie group state is updated using the exponential map of $SE(3)$ and a linear vector addition can be used for the $\mathbb{R}^4$ state.

III. Experimental Results

The IEKFs with the accelerating form of the Frenet-Serret and Bishop dynamic models are implemented in a radar tracking scenario with a target performing a trajectory comprising constant velocity, accelerating and spiralling segments. The scenario used is presented in Figure 1. The observer is

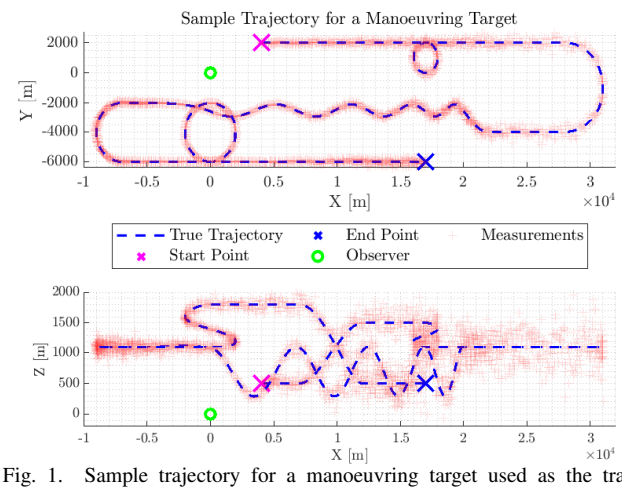

Fig. 1. Sample trajectory for a manoeuvring target used as the tracking scenario.

kept stationary for simplicity and receives range and bearing measurements at 5Hz with uncertainties of $0.01rad$ and $5m$ respectively. The filters update at 25Hz, propagating using the kinematic models when a measurement is not available. The process noises for all filters have been tuned manually.

A. Single Simulation

The FSa-LIEKF, Ba-LIEKF are implemented and compared to the FS-LIEKF and B-LIEKF. For comparison to typical algorithms used in industry, a variety of Cartesian CV and CA filters are implemented, along with the CA-CV IMM2. Figure 1 depicts a single simulation comparing the FSa-LIEKF and Ba-LIEKF to their constant velocity counterparts.. All four algorithms perform well on this trajectory but the accelerating forms show slightly reduced tracking error during the decelerating components immediately before and after the spiral manoeuvre. As expected, the FSa-LIEKF and Ba-LIEKF are able to adapt to the changing velocities faster than the constant velocity counterparts but exhibit inferior performance on zero acceleration segments. Performance on accelerating segments could be further improved at the expense of increased noise during constant velocity trajectories. In a multiple-model algorithm the accelerating model could be tuned aggressively to maximise tracking during the accelerating segment before allowing the filter to switch to a FS-LIEKF or B-LIEKF filter. Since the filters are run independently for this simulation a balance is made. Figure 3 shows the FSa-LIEKF and Ba-LIEKF responding to changes in velocity slightly faster than the filters without the norm acceleration state. As the Bishop

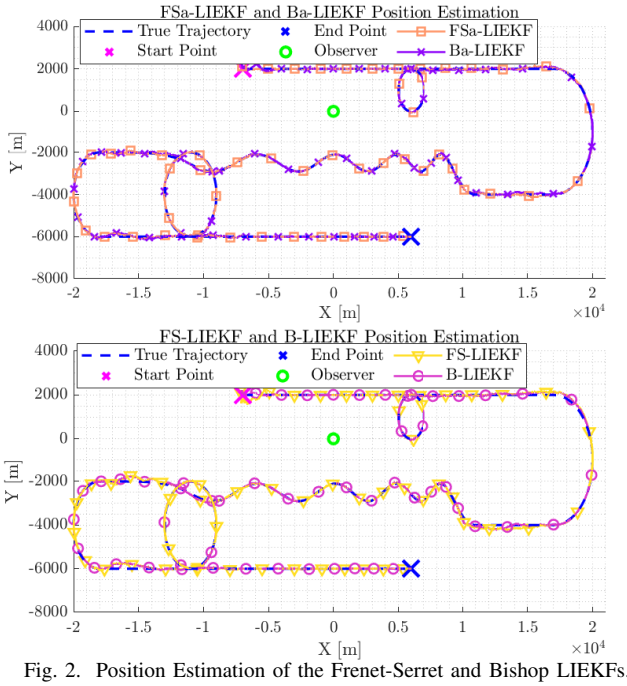

Fig. 2. Position Estimation of the Frenet-Serret and Bishop LIEKFs.

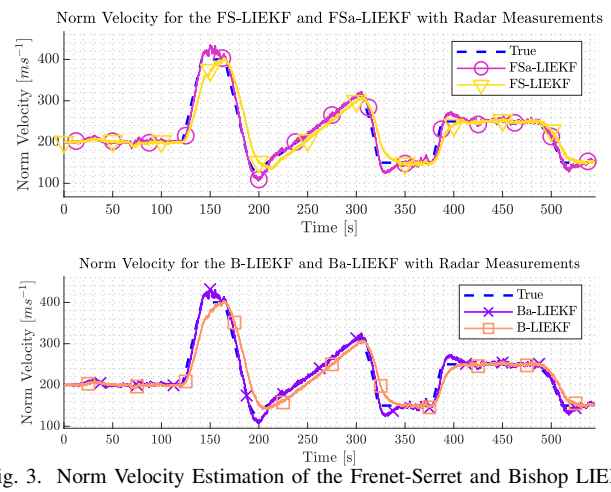

Fig. 3. Norm Velocity Estimation of the Frenet-Serret and Bishop LIEKFs.

frame to a curve is not unique, it is hard to verify the accuracy of the estimation process for the two curvatures. This is because the Bishop formulae parallel transport the frame through a minimum rotation and will therefore change dependent on the initial frame. We plot the equivalent absolute Frenet curvature κ through $\kappa = \sqrt{\kappa_1^2 + \kappa_2^2}$. This is presented in Figure 4. It should be noted that we have chosen to define the Frenet-Serret curvature as a signed scalar, with clockwise turns assigned a positive curvature. Additionally, since the filters estimate $\hat{\kappa} = u\kappa$, the state estimate is divided by the estimated norm velocity for plotting. Both Bishop filters track the equivalent Frenet-Serret curvature well and, since the tracking of the curvature is dependent on accurate estimation of both curvatures, it suggests that the Bishop frame is able to estimate both scalars more effectively than the Frenet-Serret counterparts. Norm acceleration estimation of the Ba-

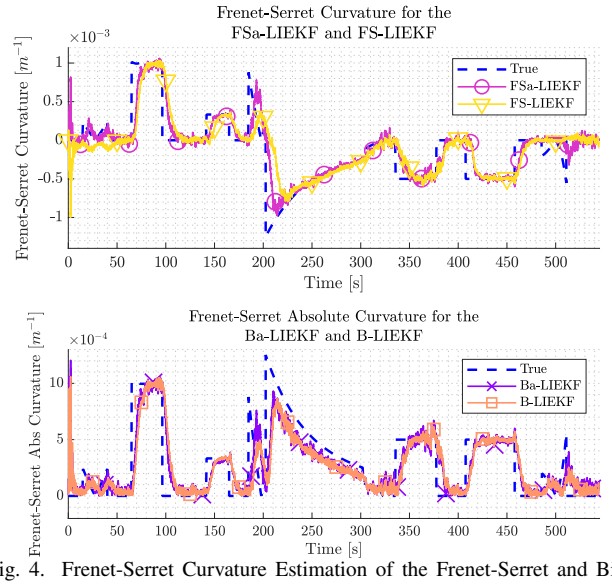

Fig. 4. Frenet-Serret Curvature Estimation of the Frenet-Serret and Bishop LIEKFs.

LIEKF and FSa-LIEKF is depicted in Figure 5 with both filters performing well, although results could be improved with more aggressive process noise at the expensive of smoother velocity estimation.

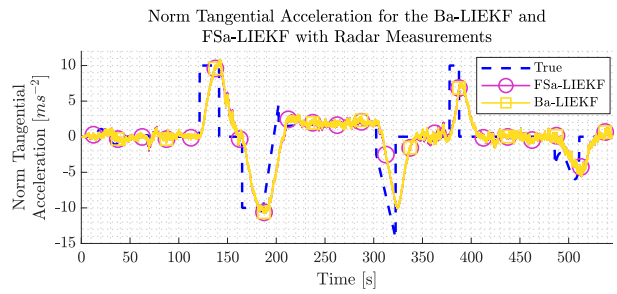

Fig. 5. Norm Tangential Acceleration Estimation of the Frenet-Serret and Bishop LIEKFs.

B. Monte Carlo Simulation

The results from a Monte Carlo analysis with 50 simulations provide a performance comparison for the IEKFs along with some basic but common industry algorithms. The root-mean-squared-errors (RMSE) of the position and norm velocity for each filter during the simulation are presented below in Tables I and II. The largest improvement in performance comes

TABLE I
LIEKF RMSEs FOR SIMULATION

State	B-LIEKF	Ba-LIEKF	FS-LIEKF	FSa-LIEKF
x	34.71	34.52	34.02	33.50
y	42.23	39.43	43.31	40.60
z	38.95	36.71	39.64	43.04
u	9.82	9.09	10.09	9.42

during manoeuvres not currently defined by the Frenet-Serret scalars, that is non-constant velocities, and it is here where both the Ba-LIEKF and FSa-LIEKF show their merits. The

TABLE II
EKF RMSES FOR SIMULATION

State	CV-EKF	CA-EKF	IMM2-EKF
x	36.48	33.66	35.02
y	60.17	43.09	42.34
z	52.93	43.77	43.35
u	15.72	14.29	13.34

FSa-LIEKF and Ba-LIEKF show marginally improved norm velocity estimation, shown in Table I, although the trajectory presented has six segments with non-zero acceleration, so it is purposely well-suited to the FSa-LIEKF and Ba-LIEKF. Increased noise is seen during trajectory elements that do not require an acceleration term. Since the Frenet-Serret and Bishop formulae already allow for a broad range of motion, the use cases for the FSa-LIEKF and Ba-LIEKF are diminished. It is therefore recommended that the accelerating forms should only be used over the B-LIEKF and FS-LIEKF when a target is known to perform a large number of accelerating manoeuvres. The CV and CA filters are not ideally suited to some of the trajectory segments that would be best tracked by a coordinated-turn (CT) model, but Table II shows the CA-EKF performing better which, given the number of manoeuvres is reasonable. The IMM2 algorithm provides robust performance using simple Cartesian models but would benefit from an additional CT or Frenet-based model.

IV. CONCLUSION

This paper has presented an extension to the Frenet-Serret and Bishop target models to account for tangential accelerations in the target kinematics. The left-invariant state error propagation matrices have been derived and implemented in LIEKF algorithms to track a manoeuvring target. The FSa-LIEKF and Ba-LIEKF are shown to be more accommodating to trajectories with accelerating components, closely tracking the changes in velocity with the detriment of increased noise during non-accelerating segments. This demonstrates that the addition of the acceleration term only improves small parts of the trajectory and the improvement on the original filters is marginal as the FS-LIEKF and B-LIEKF provide robust, single-model performance. The acceleration term also adds complexity in the tuning process and additional care is required to optimise the filter performance. Based on the simulation undertaken, the original B-LIEKF and FS-LIEKF are more than well equipped to estimate complex trajectories, and the accelerating forms would be complementary extensions in a multiple-model algorithm.

A. Future Work

With two kinematic models available for each filter, we plan on developing an invariant-IMM based on [15] or multiple-model particle filter to embed the geometric models into more complex tracking algorithms.

ACKNOWLEDGMENT

This work is partly supported by PhD funding from Leonardo UK.

REFERENCES

[1] S. Julier, J. Uhlmann, and H. F. Durrant-Whyte, "A new method for the nonlinear transformation of means and covariances in filters and estimators," *IEEE Transactions on automatic control*, vol. 45, no. 3, pp. 477–482, 2000.

[2] I. Arasaratnam and S. Haykin, "Cubature kalman filters," *IEEE Transactions on automatic control*, vol. 54, no. 6, pp. 1254–1269, 2009.

[3] R. A. Singer, "Estimating optimal tracking filter performance for manned maneuvering targets," *IEEE Transactions on Aerospace and Electronic Systems*, vol. AES-6, pp. 473–483, 1970.

[4] X. R. Li and V. P. Jilkov, "Survey of maneuvering target tracking. part i. dynamic models," *IEEE Transactions on aerospace and electronic systems*, vol. 39, no. 4, pp. 1333–1364, 2003.

[5] X. R. Li and Y. Bar-Shalom, "Performance prediction of the interacting multiple model algorithm," *IEEE Transactions on Aerospace and Electronic Systems*, vol. 29, pp. 755–771, 1993.

[6] M. Pilté, S. Bonnabel, and F. Barbaresco, "Tracking the frenet-serret frame associated to a highly maneuvering target in 3d," in *2017 IEEE 56th Annual Conference on Decision and Control (CDC)*. IEEE, 2017, pp. 1969–1974.

[7] R. L. Bishop, "There is more than one way to frame a curve," *The American Mathematical Monthly*, vol. 82, no. 3, pp. 246–251, 1975.

[8] J. Gibbs, D. Anderson, M. Macdonald, J. Russell, "Invariant extended kalman filter for tracking the bishop frame using radar measurements," in *International Conference on Radar Systems*. IET, to be published 2022.

[9] P. Marion, J. Sami, B. Silvère, B. Frédéric, F. Marc, and H. Nicolas, "Invariant extended kalman filter applied to tracking for air traffic control," in *2019 International Radar Conference (RADAR)*. IEEE, 2019, pp. 1–6.

[10] M. Pilte, "Dynamic management of tracking ressources for hyper-manoeuvring targets," Ph.D. dissertation.

[11] S. Bonnabel, "Left-invariant extended kalman filter and attitude estimation," in *2007 46th IEEE Conference on Decision and Control*. IEEE, 2007, pp. 1027–1032.

[12] A. Barrau and S. Bonnabel, "The invariant extended kalman filter as a stable observer," *IEEE Transactions on Automatic Control*, vol. 62, no. 4, pp. 1797–1812, 2016.

[13] A. Barrau and S. Bonnabel, "Invariant kalman filtering," *Annual Review of Control, Robotics, and Autonomous Systems*, vol. 1, no. 1, pp. 237–257, 2018.

[14] M. Brossard, A. Barrau, and S. Bonnabel, "A code for unscented kalman filtering on manifolds (ukf-m)," in *2020 IEEE International Conference on Robotics and Automation (ICRA)*. IEEE, 2020, pp. 5701–5708.

[15] T. L. Koller and U. Frese, "The interacting multiple model filter and smoother on boxplus-manifolds," *Sensors*, vol. 21, 6 2021.